
Introducing RSESS: An Open Source Enumerative Sphere Shaping Implementation Coded in Rust

Frederik Ritter
Andrej Rode
Laurent Schmalen

UOOGK@STUDENT.KIT.EDU
 RODE@KIT.EDU
 LAURENT.SCHMALEN@KIT.EDU

Karlsruhe Institute of Technology (KIT), Communications Engineering Lab (CEL), Hertzstr. 16, 76187 Karlsruhe

Abstract

In this work, we present an open source implementation of the enumerative sphere shaping (ESS) algorithm used for probabilistic constellation shaping (PCS). PCS aims at closing the shaping gap caused by using uniformly distributed modulation symbols in channels for which information theory shows non-uniformly distributed signaling to be optimal. ESS is one such PCS algorithm that sets itself apart as it operates on a trellis representation of a subset of the possible symbol sequences. ESS leads to an empirical distribution of the symbols that closely approximates the optimal distribution for the additive white Gaussian noise (AWGN) channel. We provide an open source implementation of this algorithm in the compiled language Rust, as well as Python bindings with which our Rust code can be called in a regular Python script. We also compare simulation results on the AWGN channel using our implementation with previous works on this topic.

1. Introduction

The capacity of a channel is defined as the maximum code rate with which reliable transmission (i.e. with vanishing error probability) is possible. On an AWGN channel, the capacity can be achieved with a continuous and normally distributed channel input (Shannon, 1948; Forney & Wei, 1989). Though this would be optimal for a continuous channel input, a discrete set of channel input symbols is used in practical communication systems. Furthermore, many communication systems employ a set of uniformly distributed, discrete symbols as channel input. As a result, the channel capacity can not be achieved. The gap to capacity caused

by using a suboptimal channel input is called shaping gap and amounts to 0.255 bit/channel use (Gültekin et al., 2020; Forney et al., 1984). In terms of signal-to-noise ratio (SNR), this corresponds to a loss of 1.53 dB in energy efficiency.

Two major approaches to reduce the shaping gap are known in literature (Sun & van Tilborg, 1993; Kschischang & Pasupathy, 1993): Geometric constellation shaping (GCS) and PCS. While GCS changes the constellation symbols and induces changes to most parts and algorithms in the communication system, PCS alters the probability of occurrence of constellation symbols placed on a rectangular, evenly spaced grid.

One difficulty with probabilistic constellation shaping is the integration with forward error correction (FEC). The de-mapping of received symbol sequences back to bit strings is sensitive to wrongly detected symbols and does not easily allow the use of soft information. In (Böcherer et al., 2015), the probabilistic amplitude shaping (PAS) architecture was introduced to mitigate this problem. It works by shaping only the amplitude of transmit symbols and the approximately uniformly distributed parity bits are used to determine the sign. At the receiver the channel decoder can use soft information to recover the shaped bits which were used to create the amplitude sequence. Therefore the amplitude sequence can be regenerated error-free and dematched to the original bit sequence. The PAS architecture combines the benefits of probabilistic shaping with the benefits of using FEC. Because this is an important improvement over plain probabilistic shaping, for the remainder of this paper we will assume the use of PAS. Therefore, further discussion will focus on mapping a sequence of bits to a sequence of amplitudes rather than to a sequence of symbols. We have to note that this approach only works for distributions which are symmetric in their amplitudes.

PCS can be subdivided into direct and indirect methods. Direct methods attempt to change the occurrence probability of the transmit symbols to a given target distribution. A prominent example of the direct method is constant composition distribution matching (CCDM). It works on fixed-

length symbol sequences by collecting into a code book only those sequences, where the relative frequency of occurrence of the symbols matches the desired probability of occurrence. Bit strings are then unambiguously assigned to the sequences in the codebook and the corresponding sequence is sent in place of a given bit string. The decoder in the receiver uses the same codebook, such that it can recover the original bit string from the received symbol sequence. Using arithmetic coding (Schulte & Böcherer, 2016), the mapping and de-mapping of CCDDM can be implemented efficiently. Unfortunately, this straightforward scheme suffers from significant rate losses if the sequence length is short. Other direct methods, like multiset-partition distribution matching (Fehenberger et al., 2019), try to alleviate this disadvantage. This paper focuses on indirect PCS methods, which induce a desired probability distribution through a sufficiently well-designed goal function. In the context of Gaussian channels, one possible goal function limits the energy of the fixed-length symbol sequences in the codebook. This approximates a Maxwell-Boltzman distribution of the symbols for large sequence lengths, which is the optimal distribution for discrete symbols (Kschischang & Pasupathy, 1993). By including all sequences with energy below a certain threshold, indirect methods create the largest possible codebook for a given average energy. As the shaping rate is proportional to the logarithm of the codebook size, they suffer the minimal rate loss achievable with a finite sequence length. By interpreting a sequence of symbols as a multidimensional vector, the energy of the sequence becomes the vectors' square norm. All sequences with their energy lower than the threshold would thus be contained in a multidimensional sphere. Hence, these methods are also called sphere shaping. There are multiple algorithms that use sphere shaping, notably: Laroia's first algorithm, shell mapping (Laroia et al., 1994), and ESS (Willems & Wuijts, 1993).

ESS uses a trellis representation of the codebook and performs the mapping to bit sequences based on a lexicographical ordering of the symbol sequences. This allows for a slight reduction in complexity compared to Laroia's first algorithm and a substantial reduction in complexity compared to shell mapping. A drawback of ESS is that the lexicographical indexing leads to slightly suboptimal results if the number of sequences is limited to a power of two. This is relevant because the number of bit sequences of a fixed length is always a power of two. (Gültekin et al., 2020)

Notation:

Amplitude shift keying (ASK) is a modulation scheme that encodes the information in multiple real symbols. Using individual ASK constellations for the inphase and quadrature branch of an IQ modulator, quadrature amplitude modulation (QAM) follows. As we are only interested in the amplitudes for shaping, we define the set of amplitudes for an

M -ASK system as

$$\mathcal{A} = \{1, 3, 5, \dots, M - 1\}.$$

A sequence of N amplitudes is denoted by $\mathbf{a}^N \in \mathcal{A}^N$. The individual amplitudes in the sequences are denoted by

$$\mathbf{a}^N = (a_0 \ a_1 \ a_2 \ \dots \ a_{N-1}).$$

We use the squared norm of an amplitude sequence to define its energy

$$E(\mathbf{a}^N) = \|\mathbf{a}^N\|^2 = \sum_{n=0}^{N-1} a_n^2.$$

The remainder of this paper is organized as follows: We first provide an overview of the ESS algorithm in Section 2. A discussion of the optimum enumerative sphere shaping (OESS) algorithm, which addresses the issue of ESS being suboptimal for fixed bit length indexes, is added in Section 3. The introduction and evaluation of RSESS, which implements ESS and OESS, follows in Section 4. Finally, the paper is summarized by Section 5.

2. Enumerative Sphere Shaping

In this section, we will briefly outline the algorithms used in ESS for mapping from a bit-sequence to a symbol sequence and vice versa. We like to refer the reader to (Willems & Wuijts, 1993) for the original idea and to (Gültekin et al., 2020) for a more detailed description.

2.1. Bit Sequence to Amplitude Sequence Mapping

To transform a stream of uniformly distributed bits into a stream of non-uniformly distributed symbols, ESS uses a fixed-to-fixed length mapping: A fixed-length sequence of bits is transformed into a fixed-length sequence of symbols. The possible symbol sequences are collected into a codebook and, as the bits are uniformly distributed, all symbol sequences in the codebook are equally likely. To achieve a non-uniform symbol distribution, the symbol sequences in the codebook have to be chosen carefully. In ESS, this is achieved by constructing a codebook of all sequences with energy less than a fixed energy threshold E_{\max} . For an infinite sequence length, the symbol distribution in this codebook converges to the Maxwell-Boltzman distribution. In addition, the average energy of the codebook is always minimal for its size, which leads to minimal rate loss. The one-to-one mapping from bit sequences to symbol sequences is obtained by lexicographical ordering of the codebook. Lexicographical ordering is the method of ordering words in a dictionary but applied to sequences of symbols. A sequence \mathbf{a}^N is said to be larger than sequence \mathbf{b}^N if there exists some

n , with $1 \leq n \leq N$ such that the symbols of both sequences below index n are equal ($a_i = b_i, i < n$) and its symbol at index n is larger than that of the other sequence ($a_n > b_n$). For example, the first sequences in the codebook for a sequence length $N = 3$ and 8-ASK are $(1\ 1\ 1)$, $(1\ 1\ 3)$, $(1\ 1\ 5)$, $(1\ 1\ 7)$, $(1\ 3\ 1)$, $(1\ 3\ 3)$ and so on. Having defined an ordering allows indexing the sequences. The index $i(\mathbf{a}^N)$ of a sequence \mathbf{a}^N is defined as the number of sequences below it. Thus with the example from above, we can state that $i((1\ 1\ 1)) = 0$, $i((1\ 1\ 3)) = 1$, $i((1\ 1\ 5)) = 2$ and so on. Due to the mapping being invertible, we can easily define the inverse mapping $\mathbf{a}^N(i)$ as the sequence with index i . Taking the energy threshold into account, not all possible sequences are contained in the codebook. Table 1 shows all amplitude sequences in the codebook for $N = 4$, $E_{\max} = 28$ and 8-ASK. Each index can be converted to its binary representation to obtain an invertible mapping from bit sequence to amplitude sequence.

Table 1. Codebook for $N = 4$ and $E_{\max} = 28$ using 8-ASK with index for each sequence according to (Gültekin et al., 2020).

i	$\mathbf{a}^N(i)$	i	$\mathbf{a}^N(i)$	i	$\mathbf{a}^N(i)$
0	(1 1 1 1)	7	(1 3 1 3)	13	(3 1 3 1)
1	(1 1 1 3)	8	(1 3 3 1)	14	(3 1 3 3)
2	(1 1 1 5)	9	(1 3 3 3)	15	(3 3 1 1)
3	(1 1 3 1)	10	(1 5 1 1)	16	(3 3 1 3)
4	(1 1 3 3)	11	(3 1 1 1)	17	(3 3 3 1)
5	(1 1 5 1)	12	(3 1 1 3)	18	(5 1 1 1)
6	(1 3 1 1)				

2.2. Bounded Energy Trellis

Storing the codebook in a lookup table (LUT), as in the example in Table 1, quickly becomes impractical for large codebooks. However, it is not necessary to explicitly store the codebook; we only require a fast way of finding how many sequences are lexicographically below a given sequence. This can be achieved by a bounded energy trellis. It consists of nodes corresponding to a number of amplitudes n and accumulated energy e . Each node T_n^e holds the number of different sequences that are still possible with n fixed amplitudes which result in the accumulated energy e . For example, by using the same base parameters as for Table 1 the node T_3^{19} has two possible continuations i.e. $T_3^{19} = 2$. As $n = 3$ amplitudes are fixed, only $N - n = 1$ amplitude can be varied. This amplitude could take the values 1 or 3. However, if it takes the value 5 or higher the total energy $e + 5^2 = 19 + 5^2 = 44$ would exceed the maximum energy $E_{\max} = 28$. Thus the number of possible continuations is two. An example trellis for $N = 4$, $E_{\max} = 28$ and 8-ASK can be seen in Figure 1. It holds

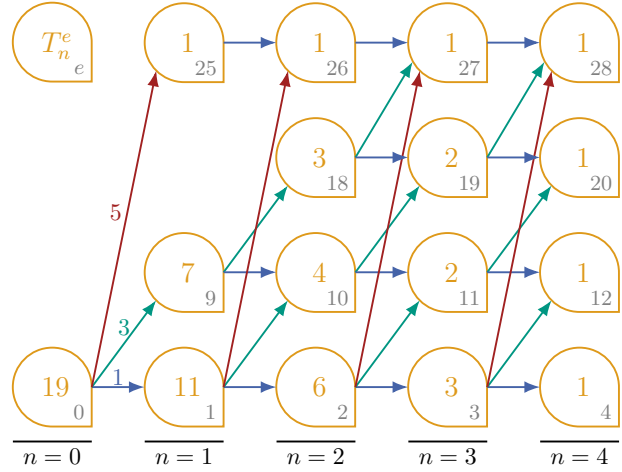


Figure 1. Bounded energy trellis diagram for $N = 4$ and $E_{\max} = 28$ and 8-ASK following (Gültekin et al., 2020).

the same codebook and results in the same mapping as Table 1. The number of accumulated energy values can be reduced by observing that the energy added by any amplitude can be written in the form $1 + k \cdot 8$. For instance, the amplitude 5 has the energy $5^2 = 25 = 1 + 3 \cdot 8$. Thus the accumulated energies after n fixed amplitudes will always be n plus a multiple of 8 and trellis nodes are only needed for these values. Of course, there must be nodes for $n = 0$ to $n = N - 1$ fixed amplitudes. There are also nodes for $n = N$ fixed amplitudes. Trivially, all of these nodes have the value 1 and the remaining values in the trellis are built up backwards from these. Assuming we have the values in all nodes with $n + 1$ fixed amplitudes, the value of a node with n fixed amplitudes is the sum of all values from nodes with $n + 1$ fixed amplitudes which are reachable by adding a single amplitude to the node. Adding an amplitude to a node means adding its energy to the accumulated energy of the node and corresponds to appending the amplitude to the sequences represented by this node. This rule holds because the value of a node is the number of different sequences possible with it as the starting point. Naturally, the number of continuations is the sum of the number of continuations after each possible next amplitude. By leveraging the fact that the nodes with $n = N$ are indeed all known to be 1, all values in the trellis can thus be calculated by applying

$$T_n^e = \sum_{a \in \mathcal{A}} T_{n+1}^{e+a^2} \quad (1)$$

recursively starting from $n = N - 1$ and down to $n = 0$.

2.3. Encoding and Decoding via the Trellis Diagram

Each amplitude sequence can be interpreted as a path through the bounded energy trellis: each transition in the

trellis is equivalent to appending an amplitude to a sequence represented by a node. For example, the amplitude sequence (1 3 3 1) corresponds to the path $T_0^0 \rightarrow T_1^1 \rightarrow T_2^{10} \rightarrow T_3^{19} \rightarrow T_4^{20}$ in the trellis diagram in Figure 1. Indexing the sequences in the trellis makes use of this path representation and the definition of the index being the number of lexicographically lower sequences. Amplitude sequences are constructed from left to right, therefore the sequences have their more significant amplitudes added first.

The index of a given sequence is defined by the lexicographical ordering but the sequence for a given index is only defined as the inverse operation. Therefore, it is best to discuss the decoding algorithm (finding the index of a given sequence) first. Indexing a sequences in the trellis makes use of its path representation by following the path one step at a time. This corresponds to “building” the sequence by appending one amplitude in each step. By keeping track of the number of sequences left lexicographically below in each step, the sum of lower sequences can be computed, which is the index. The number of sequences left below in each step is the number of sequences possible if a lower amplitude would be appended instead of the next one in the sequence. For each lower amplitude a , this number can easily be retrieved from the trellis diagram as it is the value of the trellis node reached if the lower amplitude a is used next. Thus if we are currently in the node $T_n^{e_n}$, the number of sequences possible if amplitude a is appended equals $T_{n+1}^{e_n+a^2}$. Algorithm 1 accumulates the number of possible sequences for each lower amplitude in each step to compute the index of a given sequence. For the chosen system parameters in Figure 1, the obtained indices correspond to the codebook in Table 1.

Algorithm 1 Mapping Amplitude Sequence to Index

```

input  $a^N$ 
 $e_n = \begin{cases} 0, & n = 0 \\ \sum_{j=0}^{n-1} a_n^2, & n \in \{1, \dots, N-1\} \end{cases}$ 
 $i = 0$ 
for  $n = 0$  to  $N - 1$  do
    for  $a \in \mathcal{A}; a < a_n$  do
         $i = i + T_{n+1}^{e_n+a^2}$ 
    end for
end for
output  $i$ 
    
```

Encoding, which is mapping an index to an amplitude sequence can be achieved using Algorithm 2. If the path of a full length amplitude sequence contains a node T_n^e , it also contains one of the T_n^e continuations of this node. The sequence cannot be lexicographically greater than all its continuations after the amplitude in location n . Thus the index

of a sequence with node T_n^e in its path is upper bounded by $T_n^e - 1$ plus the number of sequences left lexicographically below in the path leading up to node T_n^e . Finding the correct next node now becomes a matter of finding the lowest next amplitude such that the value of the next node plus the number of lexicographically lower sequences is greater than the index. For example, assume we are searching for the sequence belonging to index $i = 13$ using the trellis in Figure 1. We know it starts with (3 1 ? ?) and $j = 11$ sequences are lexicographically lower than this start of the sequence. Following the path or calculating the accumulated energy ($3^2 + 1^2 = 10$) shows that we are on a path that currently ends on node T_2^{10} . If the next amplitude is chosen to be 1, the next node is T_3^{11} . This will lead to an index which is too small as $j + T_3^{11} = 11 + 2 = 13 \leq 13 = i$. Thus, the next larger amplitude 3 must be tried. As all sequences continuing with 1 are lexicographically below any sequence continuing with a 3, these must be added to the number of sequences left below. The variable j is thus updated by adding $T_3^{11} = 2$, which is the number of sequences continuing with amplitude 1. The current index j now equals $11 + 2 = 13$. If the next amplitude is a 3, the next node is T_3^{19} . Now the index $i = 13$ is smaller than $j + T_3^{19} = 13 + 2 = 15$ and the next amplitude is chosen to be 3. Checking Table 1 shows that the correct sequence with index $i = 13$ is (3 1 3 1), which does indeed have a 3 in the location in question. Algorithm 2 starts from the known starting node T_0^0 and applies this method iteratively to compute the full sequence.

Algorithm 2 Mapping Index to Amplitude Sequence

```

input  $i$ 
 $a^N = (a_0 a_1 \dots a_{N-1}) \in \mathcal{A}^N$ 
 $e = 0$ 
 $j = 0$ 
for  $n = 0$  to  $N - 1$  do
     $a = 1$ 
    while  $i \geq j + T_{n+1}^{e+a^2}$  do
         $j = j + T_{n+1}^{e+a^2}$ 
         $a = \text{next larger value in } \mathcal{A}$ 
    end while
     $a_n = a$ 
     $e = e + a^2$ 
end for
output  $a^N$ 
    
```

2.4. Amplitude Distribution and Average Energy

For the purpose of evaluating the resulting code book, two metrics are especially interesting: the amplitude distribution and the average symbol energy. The amplitude distribution is defined as the probability of finding a given amplitude in a random location in a sequence chosen ran-

domly from the codebook. As ESS is an indirect method and thus uses no predefined amplitude distribution, the amplitude distribution must be calculated from the codebook. As shown in (Gültekin et al., 2020), the amplitude distribution can be calculated using the trellis representation via

$$P_A(a) = \frac{T_1^{a^2}}{T_0}. \quad (2)$$

The average energy can be computed by averaging the energy of amplitude sequences in the codebook. It is of interest because it directly influences the signal-to-noise ratio in the case of an AWGN channel. Given the amplitude distribution, the average energy

$$E_{av} = N \sum_{a \in \mathcal{A}} P_A(a) a^2 \quad (3)$$

can trivially be computed using the energies of the amplitudes and the sequence length (Gültekin et al., 2020).

3. Fixed-Length Messages and Optimum ESS

In the general case, the number of sequences in the codebook is not a power of two. This is disadvantageous as in a fixed-to-fixed distribution matcher, a fixed number of bits should be mapped to these sequences and the number of possible bit strings of any length is always a power of two. Using the binary interpretation of the bit stream as index, sequences that have an index higher than $2^{N_{\text{bit}}} - 1$ are not used. For large codebooks this disadvantage becomes negligible. For very small codebooks, however, ESS becomes less efficient than other methods. As the sequences are ordered lexicographically and not by their total energy, the sequences with the highest indices do not necessarily have the highest energy. This removes lower energy sequences from the codebook and the average energy is no longer minimal. The rate loss incurred by ESS compared to an optimal minimum average energy codebook, is hereby increased. OESS as proposed in (Chen et al., 2022) alleviates this problem.

As multiple energy thresholds E_{max} can lead to the same possible bit string length, OESS is defined for the lowest E_{max} that leads to a given bit string length. The key idea of OESS is to use two trellis diagrams instead of only one. One trellis diagram is a normal bounded energy trellis but with the threshold $E_{\text{max}} - 8$. As discussed in the previous section, the energy of amplitude sequences is quantized to multiples of eight plus an offset. Therefore, the first trellis diagram, called the full trellis in (Chen et al., 2022), contains all sequences except for those with maximum energy content E_{max} . The second trellis diagram is called the partial trellis and contains only the sequences with energy equal to E_{max} . A trellis like this can easily be constructed

by altering the values of the final trellis nodes during initialization. For a regular ESS trellis, all nodes with $n = N$ are initialized to 1. In the partial trellis used by OESS, only $T_N^{E_{\text{max}}}$ is set to 1 while all other nodes are set to 0. Applying (1) in the regular way calculates all other node values. By splitting the sequences with maximum energy into a new trellis, these are enumerated separately. Mapping an index to a sequence now works by first selecting the appropriate trellis. If the index is lower than the number of sequences in the full trellis, a sequence from the full trellis is chosen using Algorithm 2. Otherwise a local index for the partial trellis is created by subtracting the number of sequences in the full trellis from the index. Algorithm 2 is then used on the partial trellis with the local index to find the corresponding amplitude sequence with energy E_{max} . This way the highest indices correspond to sequences with maximum energy. Therefore, removing sequences which are located in the partial trellis will reduce the average energy. Demapping works in a similar way as the mapping. First, the energy of the sequence is calculated. If it is below the maximum energy, the full trellis is used with Algorithm 1 to find the index. Should the sequence have maximum energy, the local index is calculated from the partial trellis using Algorithm 1 and the number of sequences in the full trellis is added to it, which is necessary to obtain the final index from the local index computed with the partial trellis.

To calculate the amplitude distribution in OESS, we are not able to use the simple form (2). Instead, we need to apply a calculation that takes into account that some of the sequences are removed from the codebook, therefore changing the amplitude distribution. Calculation of the amplitude distribution for ESS with a limited codebook size and calculation of the amplitude distribution for OESS can be found in (Chen et al., 2022).

4. Introducing RSESS

Our contribution is a free and open source implementation of the ESS and OESS algorithms. We used the programming language Rust to implement the presented algorithms. We distribute the code in the form of a Rust crate named RSESS on crates.io. The full source code is also available at <https://github.com/kit-cel/rsess>. Encoding and decoding between indices and amplitude sequences form the core of RSESS. For analysis, calculation of the amplitude distribution is implemented both for the simple case in which all sequences are used as well as for the more complex cases in which only indexes up to a power of two are used or the amplitude distribution for OESS. Calculation of the average energy is also implemented as well as the calculation of the energy distribution, which gives the probabilities for sequences of specific energy. The programming interfaces to work with ESS or

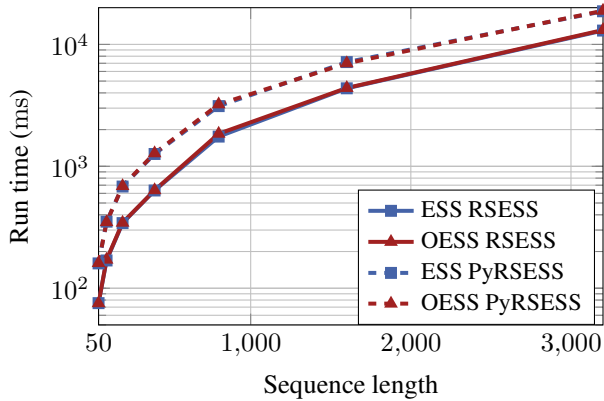


Figure 2. Encoding times over varying sequences length for 10000 sequences using our framework

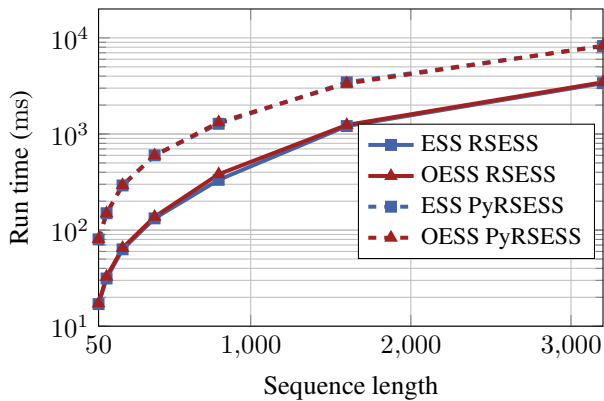


Figure 3. Decoding times over varying sequence length for 10000 sequences using our framework

OESS are identical. However, the OESS implementation features an additional function which can find the E_{\max} values for which OESS is defined. To facilitate the use in Python scripts, Python bindings for RSESS are provided in a package named PyRSESS. The source code resides in the same repository, but PyRSESS is also published to PyPI. The Python bindings cover the full scope of the Rust library.

Using a Rust or Python package manager, either RSESS or PyRSESS is easy to install. In both programming languages, we expose an object-oriented interface with one class for ESS and OESS each. Objects instantiated from these classes can be used to encode and decode bit strings into amplitude sequences and vice-versa. While RSESS uses the arbitrarily sized integers from the rust Rust crate as indices, the Python bindings use arrays/lists containing zeros and ones to model data bits. Usage examples for both RSESS and PyRSESS are also made available at https://github.com/kit-cel/rsess_examples.

The main reason for implementing the ESS algorithm in the compiled language Rust was the goal to have fast encoding and decoding. Simulations regularly calculate thou-

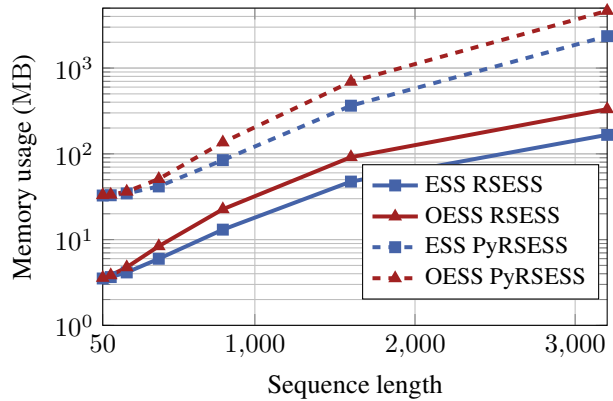


Figure 4. Resident memory over varying sequence lengths for 10000 sequences using our framework

sands of transmissions over the simulated channels and a fast implementation is invaluable in this situation. In ESS encoding/decoding, speed mainly depends on the amplitude sequence length N , the energy threshold E_{\max} , and the data itself. Together, the combination of N and E_{\max} determines the number of data bits N_{bits} . For the following benchmarks a constant shaping rate $r_{\text{sh}} = \frac{N}{N_{\text{bits}}} = 1.5$ and the minimum E_{\max} possible with this r_{sh} is used. The use of 10000 random data sequences allows statements about the data-independent average encoding / decoding behavior. This allows the amplitude sequence length N to be the only parameter influencing algorithm complexity. Figure 2 shows the duration of encoding 10000 random bit strings for different values of N and Figure 4 shows the duration of decoding the resulting amplitude sequences back into bit strings. As the main advantage of the ESS / OESS algorithm is its low rate loss for short block lengths, performance for short amplitude sequence lengths is especially relevant. Decoding times for 10000 sequences are below one second, even for very long sequence lengths up to $N \approx 1300$. Using the Python bindings PyRSESS, decoding times stay below one second for sequence lengths up to $N \approx 600$. Encoding long sequences with lengths of $N \approx 500$ is slower but still below one second. The Python bindings only keep encoding below one second for medium block lengths below $N \approx 300$. In general, decoding is faster than encoding and pure Rust is faster than using the Python bindings. Another limiting factor may be the memory space used to store the trellis. However, our benchmarks in Figure 4 show that using pure Rust, this is not the case as the total resident process memory does not exceed 100 MB even for long sequences up to $N = 1600$. All memory measurements were done directly after creating the trellis and captured the resident memory of the whole process, not only the trellis. Unlike the encoding/decoding times, the memory usage values of ESS and OESS differ. This is to be expected as OESS uses two trellises while ESS only uses one. The memory usage of

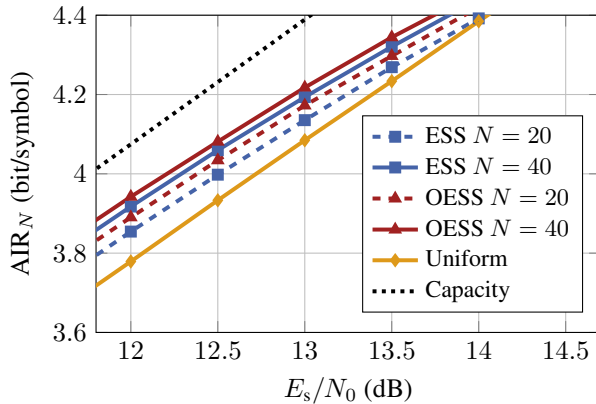


Figure 5. AIR over varying E_s/N_0 (reproducing Figure 16 in (Chen et al., 2022))

PyRSESS is much higher than that of the pure Rust library and even exceeds 2 GB for ESS with the extreme block length of $N = 3200$. OESS has even higher memory usage exceeding 4 GB, however the advantage of OESS over ESS already vanishes for far lower block lengths. We would advise against the use of PyRSESS for simulations with extremely long block lengths on hardware with limited memory resources.

Multiple simulations over an AWGN channel were conducted using PyRSESS with different sequence lengths and energy thresholds. Most notably, one simulation aimed at validating the achievable information rate (AIR) results for ESS, OESS, and CCDM at different signal-to-noise ratios published in (Chen et al., 2022). The AIR is the maximum information rate that can reliably be transmitted over a channel assuming optimal channel coding and can be estimated from the soft information before channel decoding. Using PyRSESS for the simulation of ESS and OESS, we could replicate the results published in Figure 16 in (Chen et al., 2022). Our results can be seen in Figure 5. Apart from validating the research by Yizhao Chen and colleagues, this also demonstrates that our implementations of the ESS and OESS algorithms are correct.

5. Conclusion

We have provided a short overview of probabilistic shaping and the ESS algorithm to then introduce our contribution: a free and open source implementation of ESS and OESS called RSESS. RSESS is a Rust library and also has Python bindings called PyRSESS. We have shown that RSESS is fast and memory efficient even for large simulations, while PyRSESS is an easy-to-use option for normal simulations but is less efficient and becomes demanding for very large simulations. Finally, the functionality of our implementation could be verified by replicating literature results in the short block length regime. This makes RSESS a viable tool for research and development in the field of probabilistic constellation shaping.

Acknowledgment

This work has received funding from the European Research Council (ERC) under the European Union’s Horizon 2020 research and innovation programme (grant agreement No. 101001899).

References

- Böcherer, Georg, Steiner, Fabian, and Schulte, Patrick. Bandwidth efficient and rate-matched low-density parity-check coded modulation. *IEEE Transactions on Communications*, 63(12):4651–4665, December 2015. doi: 10.1109/TCOMM.2015.2494016.
- Chen, Yizhao, Chen, Junda, Li, Weihao, Zhang, Mingming, Liu, Deming, and Tang, Ming. On optimization and analysis of enumerative sphere shaping for short blocklengths. *Journal of Lightwave Technology*, 40(22): 7265–7278, November 2022. doi: 10.1109/jlt.2022.3201901.
- Fehenberger, Tobias, Millar, David S., Koike-Akino, Toshiaki, Kojima, Keisuke, and Parsons, Kieran. Multiset-partition distribution matching. *IEEE Transactions on Communications*, 67(3):1885–1893, March 2019. doi: 10.1109/TCOMM.2018.2881091.
- Forney, G. David and Wei, Lee-Fang. Multidimensional constellations. I. Introduction, figures of merit, and generalized cross constellations. *IEEE Journal on Selected Areas in Communications*, 7(6):877–892, August 1989. doi: 10.1109/49.29611.
- Forney, G. David, Gallager, Robert G., Lang, Gordon R., Longstaff, Fred M., and Qureshi, Shahid U. Efficient modulation for band-limited channels. *IEEE Journal on Selected Areas in Communications*, 2(5):632–647, September 1984. doi: 10.1109/jsac.1984.1146101.
- Gültekin, Yunus Can, van Houtum, Wim J., Koppelaar, Arie G. C., and Willems, Frans M. J. Enumerative sphere shaping for wireless communications with short packets. *IEEE Transactions on Wireless Communications*, 19:1098–1112, 2020. doi: 10.1109/twc.2019.2951139.
- Kschischang, Frank R. and Pasupathy, Subbarayan. Optimal nonuniform signaling for Gaussian channels. *IEEE Transactions on Information Theory*, 39(3):913–929, May 1993. doi: 10.1109/18.256499.
- Laroya, Rajiv, Farvardin, Nariman, and Tretter, Steven A. On optimal shaping of multidimensional constellations. *IEEE Transactions on Information Theory*, 40(4):1044–1056, July 1994. doi: 10.1109/18.335969.

Schulte, Patrick and Böcherer, Georg. Constant composition distribution matching. *IEEE Transactions on Information Theory*, 62(1):430–434, January 2016. doi: 10.1109/TIT.2015.2499181.

Shannon, C. E. A mathematical theory of communication. *The Bell System Technical Journal*, 27(3):379–423, July 1948. doi: 10.1002/j.1538-7305.1948.tb01338.x.

Sun, Feng-Wen and van Tilborg, Henk C. A. Approaching capacity by equiprobable signaling on the Gaussian channel. *IEEE Transactions on Information Theory*, 39(5):1714–1716, September 1993. doi: 10.1109/18.259663.

Willems, Frans M. J. and Wuijts, Jos J. A pragmatic approach to shaped coded modulation. In *IEEE Symposium on Communications and Vehicular Technology in the Benelux*, 1993.